Journal of the Serbian Chemical Society
JSCS@tmf.bg.ac.rs • www.shd.org.rs/JSCS
J. Serb. Chem. Soc. *89* (3) 383–397 (2024)
JSCS–5727
Original scientific paper
Published 31 March 2024

An inverse gas chromatography study of the adsorption of organics on zeolite and zeolite/iron oxyhydroxide composite at the infinite and finite surface coverage

SLAVICA S. LAZAREVIĆ[1#]*, MARIJA T. MIHAJLOVIĆ-KOSTIĆ[2], IVONA M. JANKOVIĆ-ČASTVAN[1#], ĐORĐE T. JANAĆKOVIĆ[1#] and RADA D. PETROVIĆ[1#]

[1]*Faculty of Technology and Metallurgy, University of Belgrade, Karnegijeva 4, 11000 Belgrade, Serbia and* [2]*Belgrade Waterworks and Sewerage, Deligradska 28, 11000 Belgrade, Serbia*

(Received 8 September, revised 8 October, accepted 21 November 2023)

Abstract: The surfaces of natural (NZ) and zeolite/iron oxyhydroxide composite (ZFe) samples were analysed by means of inverse gas chromatography (IGC) using the adsorption data of organic non-polar and polar probes, in the infinite and finite-dilution regimes, in the temperature range 483–513 K. The dispersive components of the free energy of adsorption, γ_S, determined by the Gray method, decreased with increasing temperature for both zeolites. The specific interactions were characterised by the specific free adsorption energy change, ΔG_a^S, the specific enthalpy change of adsorption, ΔH_a^S, as well as the donor and acceptor interaction parameters (K_A, K_D) and the basic character of the NZ and ZFe was evidenced. The adsorption isotherms of *n*-hexane, benzene, chloroform and tetrahydrofuran (THF) were determined under finite surface coverage and used to estimate the specific surface area and the adsorption energy distribution. The adsorption capacity of the ZFe was higher than for NZ for all the investigated adsorbates. The specific surface areas and pore size distributions were also determined using nitrogen adsorption–desorption isotherms, *i.e.*, the BET method. It was observed that the nature of the adsorbate and the properties of the solid surface of the initial and modified samples governed the uptake of adsorbates.

Keywords: surface characteristics; electron donor–acceptor properties; specific surface area; adsorption energy distribution.

INTRODUCTION

Zeolites are microporous hydrated crystalline aluminosilicate minerals ($Mx / n[(AlO_2)_x(SiO_2)_y]\cdot zH_2O$, where M are alkali ($n = 1$) or alkaline ($n = 2$) earth metal

* Corresponding author. E-mail: slazarevic@tmf.bg.ac.rs
# Serbian Chemical Society member.
https://doi.org/10.2298/JSC230908093L

cation) consisting of three-dimensional structures of SiO_4 and AlO_4, tetrahedrally linked by oxygen atoms to form a structure which contains channels and cavities. Zeolites are various types of minerals that differ in their formula which generate variation in their Si/Al ratio, amount of cations, framework structure, porosity, surface area, and the surface properties (*e.g.*, hydrophobicity and acidity).[1] The isomorphous replacement of Si^{4+} by Al^{3+} results in a net negative charge that is compensated by alkali and alkaline earth metal cations within the framework. These frameworks are open so cations and water molecules have freedom of movement. As such, they are ideal molecular sieves and a high level of selectivity can be achieved in catalysis and ion-exchange. Due to their unique structure and properties (thermal stability, cage structure of molecule size, ion exchange, *etc*.) zeolites are widely used as adsorbents,[2–5] catalysts[6,7] and cation exchangers.[8,9]

The adsorption properties of natural zeolites have been improved by different physical and chemical modifications.[5] Many researchers reported that mixed systems synthesised from oxides and/or hydroxides of iron (also active adsorbents) and zeolites were able to adsorb high concentrations of inorganic species. The adsorption capacities for Mn^{2+},[10] Cu^{2+},[11] Zn^{2+},[12] and Pb^{2+},[13,14] Cd^{2+} and Zn^{2+},[15,16] As(V)[17] as well as dyes,[18,19] have been significantly increased. The desired impact of surface modification exists in the increase of specific surface area, better distribution of the particles of iron spices within the composite materials, presence of the new functional groups on the surface; ion exchange due to the presence of easily exchangeable ions; and hydroxide precipitation caused by the higher point of zero charge of the modified zeolite compared to natural zeolite.[16] But, the effect of chemical modification on their surface energy has been rarely reported.

Inverse gas chromatography (IGC) is a gas phase technique that provides information on the thermodynamic, surface energy, morphological parameters (such as, surface area and porosity), acid–base properties, glass transition temperatures, surface energy heterogeneity and reaction kinetics associated with gas––solid adsorption and catalytic reactions. In addition, the adsorption characteristics, such as isotherms and heats of adsorption, can be obtained from chromatographic experiments. The term “inverse” refers to reversal of the usual roles of the stationary and mobile phases used in conventional gas chromatography. In inverse gas chromatography, the stationary phase of the chromatographic column (solid material, such as a powder, fibre or film placed in a column) is of interest, in contrast to conventional gas chromatography when the mobile phase is the subject of interest. This stationary phase is then characterised by monitoring its interaction with volatile probe molecules of known properties as they are carried through the column *via* an inert gas. IGC has been widely used to study surface properties of various materials, such as synthetic and biological polymers, copolymers, polymer blends, adsorbents, foods, carbons, clays and catalysts.[20]

The present work was devoted to a detailed analysis of the interactions of natural and of iron oxyhydroxide modified zeolite with organic molecules from the gaseous phase at zero and finite surface coverage using inverse gas chromatography. The retentions of organic compounds of different chemical nature and polarity (non-polar, polar, donor or acceptor) were measured in the temperature range 483–513 K. The objectives of this study were to estimate and to compare: *i*) the thermodynamic parameters of adsorption (enthalpy and entropy), the dispersive and specific interactions of various organics with zeolite samples under infinite surface coverage, *ii*) the acid/base constants of zeolite samples, which describe the ability of a surface to act as electron acceptor or donor; *iii*) the adsorption isotherms and adsorption energy distributions for the adsorption of hexane, benzene, chloroform and tetrahydrofuran onto examined zeolites under finite surface coverage.

EXPERIMENTAL

Natural zeolite (NZ) from the Slanci locality, Serbia, and zeolite modified by iron(III) (ZFe) were used as adsorbents. The natural zeolite contained clinoptilolite as the dominant phase with lower contents of quartz and feldspar. The ZFe was prepared by the addition, under stirring, of 180 mL of 5 M KOH solution to a suspension of 20.0 g of natural zeolite and 100 mL of freshly prepared 1 M $FeCl_3$ solution, according to the method applied for synthesised pure goethite.[11,21] The suspension was diluted with deionized water to 2 L and held in a closed polyethylene flask at 70 °C for 60 h. The obtained brown–reddish precipitate was centrifuged, washed to remove Cl^- and dried at 105 °C. X-Ray diffraction analysis showed lower crystallinity of ZFe in comparison to the parent zeolite, and also that the ZFe contained an amorphous iron phase. According to the results of characterisation and properties, presented in the previous work,[15] it was assumed that an iron oxyhydroxide, phase similar to goethite, but not crystalline, was formed on the zeolite.

The specific surface areas and pore size distributions of the NZ and ZFe were estimated from nitrogen adsorption–desorption isotherms determined using a Micrometrics ASAP 2020 instrument. Before the measurements, the NZ and ZFe were degassed at 240 °C (the highest IGC experimental temperature) for 10 h under reduced pressure. The specific surface areas of samples (S_{BET}) were calculated according to the Brunauer, Emmett, Teller (BET) method from the linear part of the nitrogen adsorption isotherm.[22] The total pore volume (V_{tot}) was given at $p/p_0 = 0.998$. The volume of the mesopores and pore size distribution were analysed according to the Barrett, Joyner and Halenda method from the desorption isotherm.[23] The volume of the microspores was calculated according to *t*-plot analysis[24] using the Harkins–Jura thickness curve.

The following test compounds, purchased from various commercial suppliers, were used as IGC adsorbates: *n*-pentane, *n*-C_6H_{14}, *n*-heptane, *n*-octane, $CHCl_3$, diethyl ether (DEE), ethyl acetate (EtAc), THF, cyclohexane and C_6H_6. All test compounds were of HPLC grade.

IGC measurements were performed on a Perkin Elmer 8700 gas chromatograph equipped with a flame ionization detector (FID). Stainless steel columns with passivated inner walls (50 cm long and 30 cm long, internal diameter of 2.2 mm) were packed with 1.68 g of NZ (in the first series of experiments) and with 1.02 g of ZFe (in the second series of experiments). The two ends of the columns were plugged with silane-treated glass wool. Before the adsorption test of the probes, the columns were stabilised overnight on the GC system at the working

temperature under a nitrogen flow without connection to the detector in order to avoid detector contamination.

High purity nitrogen was used as the carrier gas at a flow rate of 3 cm^3min^{-1} for NZ and 6 $cm^3\ min^{-1}$ for ZFe, measured with a soap bubble flowmeter and corrected for the pressure drop in the column using a pressure gradient correction factor (j). The measurements were performed in the temperature range 483–513 K. The injector and the detector temperature were set at 563 and 593 K, respectively.

For the IGC measurements under infinite dilution conditions, minor amounts of gaseous solutes were injected manually, at least in triplicate, which permitted the lateral interactions between adsorbed molecules to be neglected. The chromatograms were collected and the retention volumes determined as the difference between the peak maxima and the column "dead time", measured with methane as a non-interacting marker. In the case of finite surface coverage, amounts from 0.5 to 10 μl of n-C_6H_{14}, C_6H_6, $CHCl_3$ and THF were injected. The retention times and peak areas were based on the average of several injections of each sample.

RESULTS AND DISCUSSION

The specific surface area was measured by the conventional nitrogen adsorption–desorption technique. Adsorption–desorption isotherms at −196 °C on NZ and ZFe and pore volume and pore size distribution are presented in Fig. 1. The measured BET surface area, mesopores and micropores volume, the overall pore volume and D_{max} – the pore size at which the density of the pore size distribution achieves its maximum and D_{ave} – the average pore diameter are given in Table I.

The ZFe sample showed a hysteresis pattern, which was associated with the filling and emptying of the mesopores by capillary condensation, but did not show a plateau at high p/p_0 values. The hysteresis loop is of type H3. The type of hysteresis pattern indicates the presence of slit-like pores.[25] The shape of the nitrogen isotherm for ZFe is characteristic for Type IIb, indicating that the material contained both mesopores, which are responsible for the hysteresis, and macropores, which results in the absence of plateau-like mesoporous Type IV isotherms.[22] The obtained t-plot for ZFe indicates that no micropores were present. The NZ sample showed a low adsorbed volume at low and intermediate relative pressures, indicating a small contribution of micropores to the total pore volume (which was confirmed by t-plot analysis), but a high adsorbed volume and a hysteresis at higher relative pressures. According to Kuila and Prasad[25] the isotherm shape indicates that NZ had negligible micropores and fine mesopores but had a significant volume of larger mesopores and macropores.

The obtained chromatographic peaks for NZ and ZFe were symmetric and had maxima independent of the amount injected, which indicated that the adsorption occurred at zero surface coverage when the lateral interactions between the molecules adsorbed at the surface can be neglected. The net retention volumes, V_N, were calculated according to Eq. (S-1 of the Supplementary material to this paper) and used for the determination of the adsorption enthalpy change, ΔH_a, and adsorption entropy change, ΔS_a (Table II). Generally, more negative values of ΔH_a

correspond to stronger interactions between the adsorbate and adsorbent. As was expected, the ΔH_a values for the *n*-alkane homologous series increased with the chain length, the molecular weight, the boiling points, and the molar refraction for both zeolite samples, NZ and ZFe (Table II). It is evident from the data in Table II that C_6H_6 exhibited a more negative ΔH_a value than the corresponding values for the aliphatic and alicyclic hydrocarbons (*n*-C_6H_{14} and *c*-C_6H_{12}), probably because of the interactions occurring between the π-electrons in the aromatic rings and the surface functional groups. Similar results were found by Diaz *et al.*[26] for the adsorption of *c*-C_6H_{12}, C_6H_6 and *n*-C_6H_{14} onto zeolite 5A and zeolite 13X.

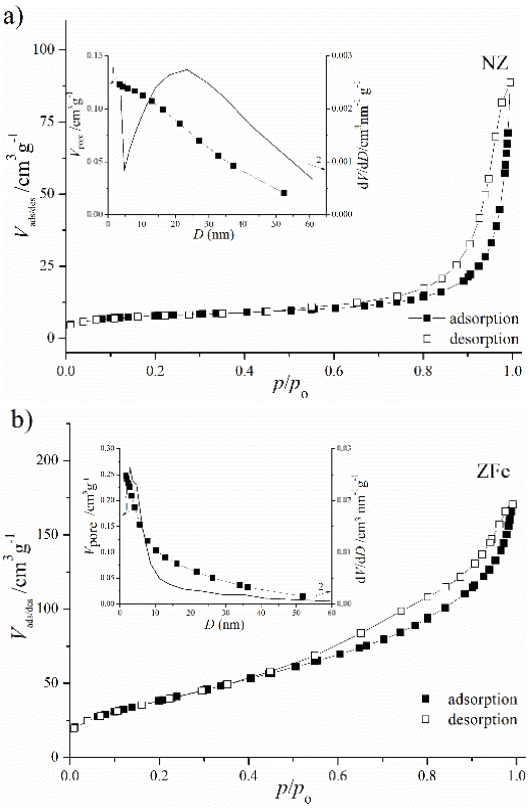

Fig. 1. Nitrogen adsorption/desorption isotherms, pore volume (1) and pore size distribution (2) of NZ (a) and ZFe (b).

The adsorption enthalpies for *n*-alkanes were higher in the case of the ZFe. According to the values of the adsorption enthalpies (Table II) the NZ sample exhibited some larger interactions with DEE, THF, C_6H_6 and *c*-C_6H_{12}, as a result of the presence of Lewis acid and Lewis base sites, whereas the ZFe samples showed stronger interactions with $CHCl_3$ and EtAc, suggesting an increase in donor properties by the formation of layers of iron oxyhydroxide on the surface and in the zeolite structural channels. During the modification, the dimensions of

the channels decreased and some acceptor sites were blocked, resulting in weaker interactions of cyclic and aromatic molecules with the ZFe.

TABLE I. The textural properties of the zeolites (240 °C)

Sample	S_{BET} $m^2 \cdot g^{-1}$	$V_{pore,total}$ $cm^3 \cdot g^{-1}$	$V_{micro,pore}$ $cm^3 \cdot g^{-1}$	$V_{meso,pore}$ $cm^3 \cdot g^{-1}$	D_{max} nm	D_{avg} nm
NZ	27.7	0.126	0.0054	0.123	23.3	20.9
ZFe	143	0.256	0.005	0.248	2.89	6.02

TABLE II. Enthalpy change of adsorption ΔH_a, and entropy change of adsorption ΔS_a, on the NZ and ZFe

Adsorbate	NZ		ZFe	
	$-\Delta H_a$ / kJ mol^{-1}	$-\Delta S_a$ / J mol^{-1} K^{-1}	$-\Delta H_a$ / kJ mol^{-1}	$-\Delta S_a$ / J mol^{-1} K^{-1}
n-C_5H_{12}	13.89	13.3±0.1	17.75	19.4±0.1
n-C_6H_{14}	18.48	19.5 ±0.1	22.97	24.1±0.1
n-C_7H_{16}	21.80	23.3±0.1	27.17	26.0±0.1
n-C_8H_{18}	26.89	30.2±0.1	33.43	32.4±0.1
$CHCl_3$	22.00	25.8±0.2	138.4	267±0.5
EtAc	27.63	21.6±0.1	45.40	56.8±0.2
DEE	33.01	32.3±0.1	20.58	6.70±0.1
THF	37.81	31.4±0.2	20.64	8.70±0.1
c-C_6H_{12}	18.43	18.7±0.1	15.00	8.20±0.1
C_6H_6	52.64	78.4±0.2	50.00	63.4±0.1

The data obtained from the interactions of the zeolite surfaces with *n*-alkanes were used to calculate the dispersive component of the surface free energy, γ_S^d, according to Eq. (S-5) of the Supplementary material. The values of ΔG_{CH2} for different temperatures were calculated as the slopes of the dependences of ΔG_a for *n*-alkanes, calculated according to Eq. (S-2), on the number of carbon atoms in the alkanes, n_C (Fig. 2). As expected, the values of ΔG_a for *n*-alkanes increased linearly with the chain length. The calculated γ_S^d values for NZ were 17.89 mJ m^{-2} at 513 K, 18.37 mJ m^{-2} at 503 K, 19.17 mJ m^{-2} at 493 K and 20.54 mJ m^{-2} at 483 K while for ZFe values were 76.73 mJ m^{-2} (513 K), 77.11 mJ m^{-2} (533 K), 77.18 mJ m^{-2} (493 K) and 77.24 mJ m^{-2} (483 K).

The γ_S^d values for both investigated samples gradually decreased with increasing temperature in the investigated range, whereby the influence of temperature was greater for NZ than for ZFe. This decrease was attributed to the entropic contribution to the surface free energy change. The γ_S^d values for the NZ sample were similar to those reported in the literature,[27,28] while the γ_S^d values for ZFe were higher than those obtained for NZ. As in the case of the ΔH_a values for *n*-alkanes, the higher values of γ_S^d for ZFe in comparison to those for NZ indicated stronger bonds between *n*-alkanes and the surface functional groups of ZFe than with surface of NZ. This could be the result of the existence of structural

heterogeneities on the lateral surface, into which linear alkanes are inserted, as well as the differences in structure, surface area and porosity due to the presence of iron oxyhydroxide in the modified sample.

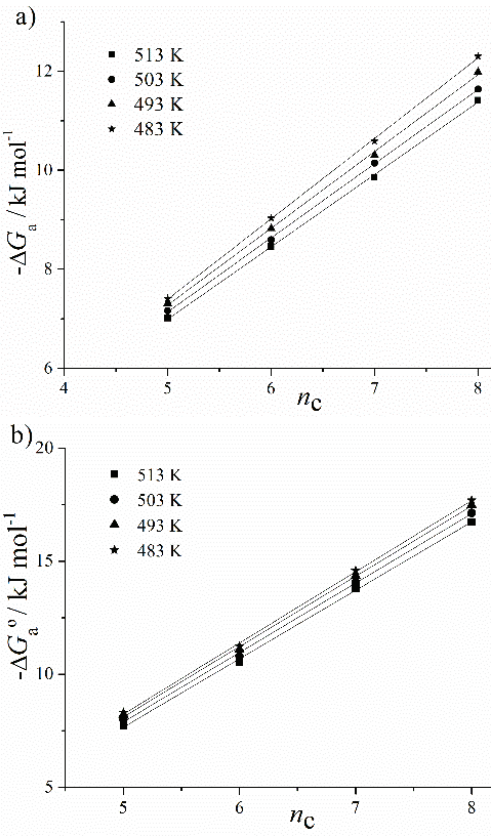

Fig. 2. Plots of ΔG_a *vs*. carbon number of *n*-alkanes for: a) NZ and b) ZFe.

The plot of $-\Delta G_a$ *versus* T_b in the case of *n*-alkanes is straight line, the "alkane line" (Figs. S-1 and S-2 of the Supplementary material). Due to specific interactions, the ΔG_a values for the polar probes are located off the alkane straight line in the dependence of ΔG_a on the adsorbate boiling point, T_b. The specific component of the free energy of adsorption (Table III) was determined from the difference between the free energy of adsorption for a polar probe and the free energy of adsorption for a real or hypothetical *n*-alkane with the same boiling point, T_b. The values presented in Fig. 3 and Table III indicate that the examined powders interact specifically with both a strong acid ($CHCl_3$) and a strong base (THF), exhibiting thereby both donor and acceptor character.

It is obvious that interactions of ZFe with polar probes are stronger than those of NZ, which indicates that the functional groups on the ZFe surface are more polar

than those on the NZ surface. Furthermore, the specific interactions are higher for the aromatic ring (C_6H_6) than for cycloalkanes. When benzene adsorbs on zeolites, there are two kinds of adsorption sites, *i.e.*, Lewis acid sites (hydroxyl protons covalently bonded to oxygen atoms bridging the framework silicon and aluminium atoms and cationic extra framework aluminium species Al^{3+}, $Al(OH)^{2+}$, and $Al(OH)^{2})^{29}$ interact with the benzene ring, and Lewis base sites, oxygen atoms in the zeolite structure, which have a very high interaction with benzene.

TABLE III. The specific free adsorption energy change ($-\Delta G_a^S$) at 513 K and $-\Delta H_a^S$ values of polar probes for NZ and ZFe

Adsorbate	NZ	ZFe	NZ	ZFe
	$-\Delta G_a^S$ /kJ mol^{-1}	$-\Delta G_a^S$ /kJ mol^{-1}	$-\Delta H_a^S$ /kJ mol^{-1}	$-\Delta H_a^S$ /kJ mol^{-1}
$CHCl_3$	6.12	19.0	25.9	34.7
EtAc	8.29	22.7	59.1	67.9
DEE	16.5	30.4	42.2	43.5
THF	15.5	27.3	42.0	40.0
c-C_6H_{12}	4.28	15.0	24.7	32.4
C_6H_6	8.04	21.9	59.0	67.5

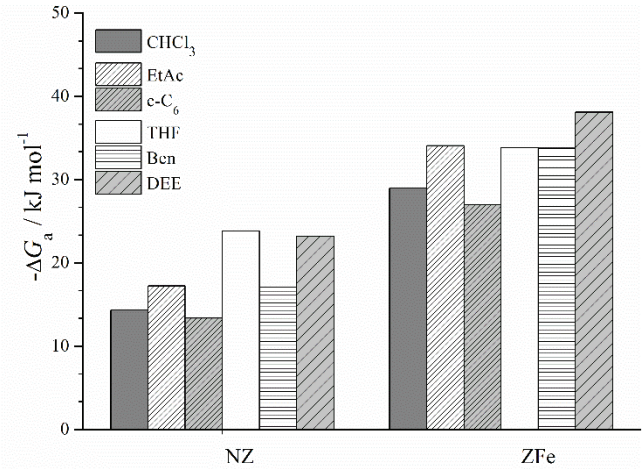

Fig. 3. The free energy change of adsorption (ΔG_a) of the polar probes on NZ and ZFe at 513 K.

The values of the specific enthalpy change of adsorption, ΔH_a^S for polar adsorbates (Table III) were obtained by plotting $\Delta G_a^S/T$ *versus* $1/T$ and used for the determination of the acid constant, K_A, and basic constant K_D according to Eq. (S-8) (Fig. 4). The determined values of K_D and K_A were 2.01 and 0.458 for NZ and 2.97 and 0.413 for ZFe.

The influence of the modification on surface properties of the NZ was confirmed by the values of K_D and K_A. The surface of the NZ exhibited predominantly

basic character with a K_D/K_A ratio of 4.39, but surface of the ZFe showed a higher basic character with the ratio of K_D/K_A = 7.20.

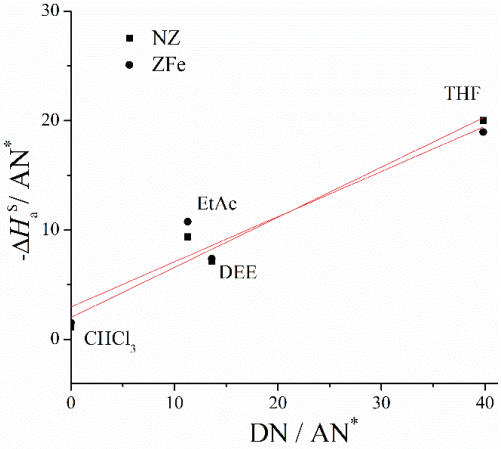

Fig. 4. Plot of $-\Delta H_a^S$ / *AN** *versus* DN/ /AN* for the adsorption of polar probes onto NZ and ZFe.

Basic constant K_D is higher and acid constant is lower for ZFe than for NZ. This is the result of the presence of basic Fe–OH groups on ZFe surface due to deposition of Fe-oxyhydroxide during the modification. The acid–base properties of the natural zeolite was in good agreement with those reported for zeolites MgY (basic character, K_D/K_A = 3.50) and NH4Y (basic character, K_D/K_A = 2.61) reported by Bilgic.[27] It should emphasize that both samples interacted strongly with chloroform, which is both an electron donor and electron acceptor. This confirms that apart from having strong donor sites, there are some sites with acceptor properties on the surfaces of the zeolites.

The adsorption behaviour of the natural and modified zeolite samples as a function of both temperature and pressure was investigated by IGC under finite conditions. The adsorption isotherms for *n*-C_6H_{14}, C_6H_6, $CHCl_3$ and THF, plotted as α (mol kg^{-1}) *versus* p (kPa), obtained at the temperature 483, 493, 503 and 513 K, are presented in Figs. 5 and 6, for NZ and ZFe, respectively.

The experimental isotherms were interpreted using the BET equation and the BET fit is represented by dotted lines. The BET plots in the indicated range gave excellent linearity for each adsorbate and for both samples. Monolayer capacity α_m and the BET constant, C, were estimated using the slope and intercept of the corresponding straight lines and listed in Table IV. The α_m values were used for the calculation of the specific surface areas of the zeolites according to Eqs. (S-13) and (S-14) (Table IV).

The adsorption capacity of the ZFe increased for all investigated adsorbates. This was expected because of the higher surface area of ZFe in comparison to NZ

and stronger interactions of used organic molecules with the new functional groups on the ZFe surface, which was proven by ΔG_a determination at infinite coverage.

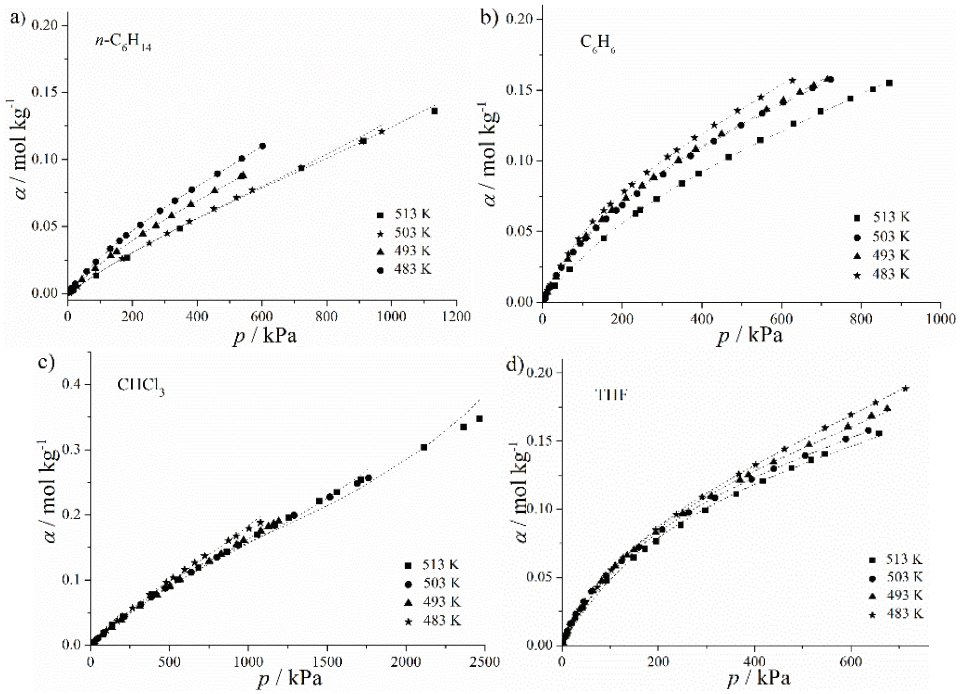

Fig. 5. Adsorption isotherms for: a) *n*-C_6H_{14}, b) C_6H_6, c) $CHCl_3$ and d) THF on the NZ at 483–513 K.

The adsorption capacity of the zeolite increased after modification for all investigated adsorbates. This was expected because of the higher surface area of ZFe in comparison to NZ and stronger interactions of used organic molecules with the new functional groups on the ZFe surface, which was proven by ΔG_a determination at infinite coverage.

According to the results presented in Table IV, the adsorption capacities of the NZ and ZFe decreased in the following order: $CHCl_3$, THF, C_6H_6 and *n*-C_6H_{14}. Previous IGC measurements at zero surface coverage showed the basic character of the NZ and ZFe. $CHCl_3$, as expected, had the greatest affinity towards the zeolites surfaces due to strong acid–base interactions and high values of the monolayer capacities were obtained. On the other hand, THF as a strong base is expected to establish repulsive forces with the zeolite surface. However, the values of monolayer capacity for THF adsorption were high for both the NZ and ZFe. Obviously, despite the fact that the surfaces of the NZ and ZFe have dominantly a basic character, there are also acid centers that interact with the strong base. A

similar conclusion was reached according to the determined acid/base properties of the NZ and ZFe at zero surface coverage.

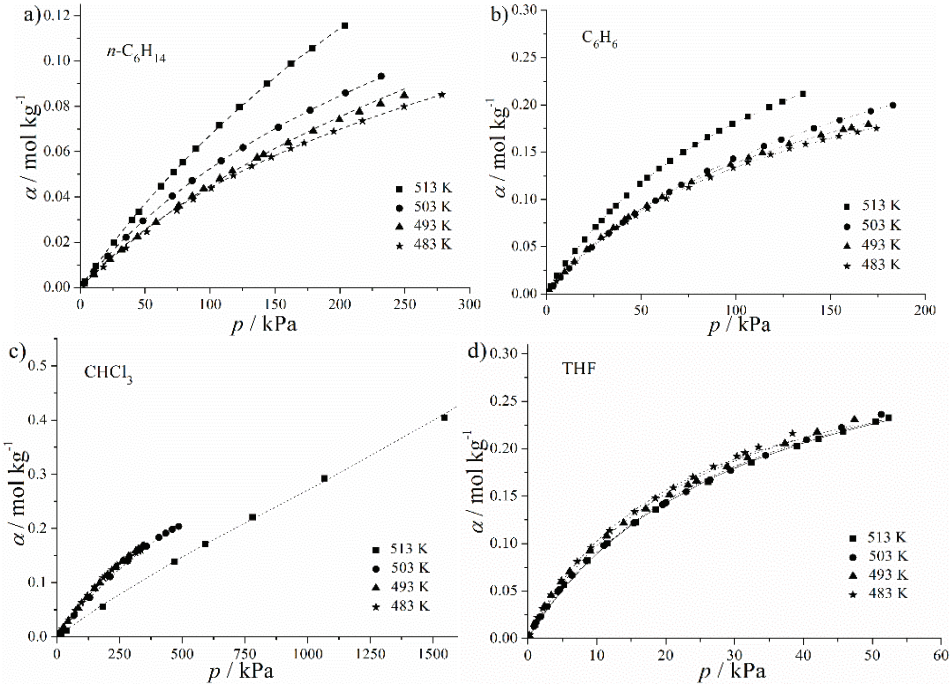

Fig. 6. Adsorption isotherms for: a) n-C_6H_{14}, b) C_6H_6, c) $CHCl_3$ and d) THF on the ZFe at 483–513 K.

Comparing the specific surface areas obtained by IGC and by the standard nitrogen adsorption method (Table I), it could be seen that the data for the NZ agree reasonably well. However, in the case of the ZFe sample, the specific surface area calculated from the IGC data obtained with n-C_6H_{14}, C_6H_6, THF and $CHCl_3$ were much lower than those obtained from nitrogen adsorption. This could be explained by differences in the molecular size. The nitrogen molecule, due to its smaller size (N_2 cross-sectional area is 0.162 nm^2), can penetrate into pores that are inaccessible to the larger molecules of n-C_6H_{14}, C_6H_6, THF and $CHCl_3$ (pore diameter of Fe–zeolite < diameter of molecule used). In the case of NZ, the mesopores were larger (the average pore diameter was 20.9 nm) and approachable for interaction with the organic probes.

The commonly accepted quantitative measure for the heterogeneity of the surface energetics, the adsorption energy distributions function, χ, that is related to the isotherm $\alpha(p,T)$, were determined using Eq. (S-15). The calculated distribution function was dependent on the choice of the local isotherm, as well as on the probe molecule.

TABLE IV. BET equation constant, C, monolayer capacity, α_m, and specific surface area of NZ and ZFe in the temperature range 483–513 K

Adsorbate	T / K	α_m / mol kg^{-1}		C		S_a /m^2 g^{-1}	
		NZ	ZFe	NZ	ZFe	NZ	ZFe
n-C_6H_{14}	513	0.121	0.268	4.30	9.34	28.7	64.0
	503	0.114	0.159	4.30	11.6	26.6	37.8
	493	0.110	0.153	5.20	8.74	26.2	36.4
	483	0.109	0.116	5.79	10.9	26.0	27.8
C_6H_6	513	0.146	0.350	7.87	29.3	26.9	64.1
	503	0.146	0.308	9.80	20.7	26.8	56.1
	493	0.135	0.258	9.90	23.6	24.8	47.2
	483	0.134	0.238	9.96	22.1	24.6	43.7
$CHCl_3$	513	0.170	0.372	7.73	3.98	28.9	63.5
	503	0.168	0.369	5.57	6.33	28.6	62.8
	493	0.167	0.357	4.40	6.25	28.5	60.8
	483	0.164	0.319	4.22	6.40	28.0	54.4
THF	513	0.163	0.352	13.86	117	28.3	61.0
	503	0.159	0.351	13.67	106	27.5	60.6
	493	0.159	0.331	12.31	112	27.5	57.2
	483	0.158	0.314	10.67	111	27.4	54.7

The distribution functions of the adsorption energy of the adsorption sites, relating the number of sites with a given energy to discrete adsorption energy values, measured with *n*-C_6H_{14}, C_6H_6, THF and $CHCl_3$ at 513 K are presented in Fig. 7a and b for the NZ and ZFe, respectively. Similar trends in the distribution functions of the adsorption sites were observed for both zeolite samples. As it could be seen from the plots that the number of adsorption sites with certain energy increased with decreasing ε_E. The obtained dependencies varied from one solid/ /adsorbate pair to another in terms of shape and the site number.

Similar values for the number of adsorption sites available on ZFe and on NZ were obtained for all four adsorbates, which suggest that number of sites on the zeolite surface did not change significantly during modification. The adsorption sites for the NZ and ZFe were also of similar energies.

The curve that describes the heterogeneity function for $CHCl_3$ was higher than that for the other adsorbates (see Fig. 6), indicating that a larger number of adsorption sites were involved in the interaction with $CHCl_3$. This is probably the result of the strong acid–base interactions of the hydroxyl groups of the adsorbate with the probe. Generally, χ is not only a characteristic of the solid itself but is also strongly dependent on the type of the solid/adsorbate combination.

The performed comparison of the adsorption energy distribution function, χ, for diverse sorbents enabled an evaluation of the heterogeneity of the surface energetics of these sorbents. The investigated samples, in spite of differences in porosity and sorption activity, were fairly similar in their degree of heterogeneity of the surface.

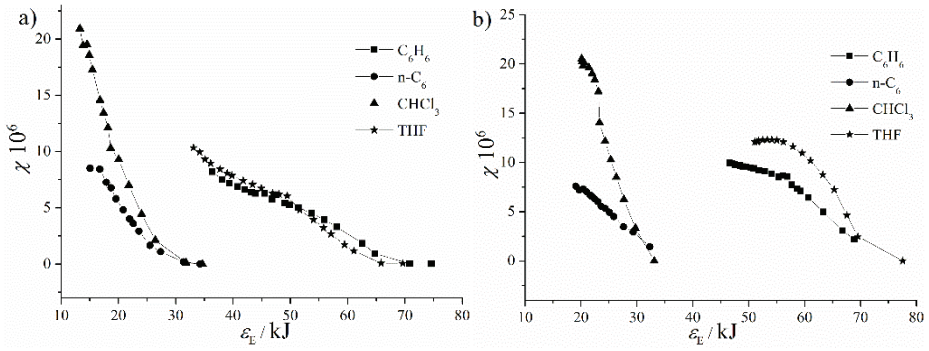

Fig. 7. Distribution functions of the adsorption sites measured with *n*-C_6H_{14}, $CHCl_3$, THF and C_6H_6 at 513 K for: a) NZ and b) ZFe.

CONCLUSION

Inverse gas chromatography under finite and infinite conditions was used to determine the surface properties of natural zeolite (NZ) and the influence of the modification with iron oxyhydroxide on the surface properties of the zeolite (sample ZFe).

Modification of the NZ considerably increased the dispersive component of its surface energy, specific interaction with polar probes, as well as the adsorption capacity for all investigated polar probes. Of the four adsorbates studied by finite coverage IGC, $CHCl_3$ had the greatest affinity towards the investigated zeolite surfaces due to strong acid–base interactions.

The NZ and ZFe strongly interacted with both the electron donor and the acceptor probes, as well as with the amphoteric probes. Based on the acceptor and donor interaction constants (K_D and K_A values), the NZ and ZFe were found to have a basic character.

The value of S_a for the NZ calculated from IGC data were in good agreement with those determined by the BET method. On the contrary, in the case of ZFe, these results did not correlated successfully due to the differences in the molecular sizes of the examined polar probes and nitrogen, as well as to the adsorbate–adsorbent interactions.

SUPPLEMENTARY MATERIAL

Additional data and information are available electronically at the pages of journal website: https://www.shd-pub.org.rs/index.php/JSCS/article/view/12579, or from the corresponding author on request.

Acknowledgment. This work was supported by the Ministry of Science, Technological Development and Innovation of the Republic of Serbia through the project contract No. 451--03-47/2023-01/200135.

ИЗВОД

ПРИМЕНА ИНВЕРЗНЕ ГАСНЕ ХРОМАТОГРАФИЈЕ ПРИ НУЛТОЈ И КОНАЧНОЈ ПРЕКРИВЕНОСТИ ЗА ИСПИТИВАЊЕ АДСОРПЦИЈЕ ОРГАНСКИХ МОЛЕКУЛА НА ЗЕОЛИТУ И КОМПОЗИТУ ЗЕОЛИТА И ГВОЖЂЕ-ОКСИХИДРОКСИДА

СЛАВИЦА С. ЛАЗАРЕВИЋ[1], МАРИЈА Т. МИХАЈЛОВИЋ-КОСТИЋ[2], ИВОНА М. ЈАНКОВИЋ-ЧАСТВАН[1], ЂОРЂЕ Т. ЈАНАЋКОВИЋ[1] и РАДА Д. ПЕТРОВИЋ[1]

[1]*Технолошко–металуршки факултет Универзитета у Београду, Карнегијева 4, 11 000 Београд и* [2]*Београдски водовод и канализација, Делиградска 28, 11000 Београд*

Применом инверзне гасне хроматографије, испитана су површинска својства природног зеолита (NZ) и композита зеолита и гвожђе-оксихидроксида (ZFe), коришћењем поларних и неполарних проба у условима нулте и коначне прекривености у температурном опсегу 483–513 K. Вредности дисперзивне компоненте слободне енергије адсорпције, γ_S, одређене методом Греја, опадају са порастом температуре за оба зеолита. Одређивањем промене специфичне слободне енергије адсорпције, ΔG_a^S, и промене специфичне енталпије адсорпције, ΔH_a^S, које одговарају кисело/базним интеракцијама на чврстој површини, одређени су и акцепторски и донорски параметри (K_A и K_D) на основу којих је утврђено да су површине узорака NZ и ZFe базног карактера. На основу добијених адсорпционих изотерми за *n*-хексан, бензен, хлороформ и тетрахидрофуран, применом инверзне гасне хроматографије у условима коначне прекривености, израчунате су вредности специфичне површине као и расподела адсорпционе енергије. Капацитет адсорпције узорка ZFe је био већи у односу на капацитета узорка NZ, за све испитане адсорбенте. Специфична површина узорака као и расподела величине мезопора одређени су применом адсорпционе/десорпционе изотерме за гасовити азот, односно применом BET методе. Закључено је да су природа адсорбата и површинска својства адсорбената главни фактори који одређују капацитет адсорпције.

(Примљено 8. септембра, ревидирано 8. октобра, прихваћено 21. новембра 2023)

REFERENCES

1. M.O. Daramola, E.F. Aransiola, T.V. Ojumu, *Materials* **5** (2012) 2101 (https://doi.org/10.3390/ma5112101)
2. N. Finish, P. Ramos, E. J.C. Borojovich, O. Zeiri, Y. Amar, M. Gottlieb, *J. Hazard. Mater.* **457** (2023) 131784 (https://doi.org/10.1016/j.jhazmat.2023.131784
3. D. Nibou, H. Mekatel, S. Amokrane, M. Barkat, M. Trari*, J. Hazard. Mater.* **173** (2010) 637 (https://doi.org/10.1016/j.jhazmat.2009.08.132)
4. V. Yadav, L. Kumar, N. Saini, M. Yadav, N. Singh, V. Murugasen, E. Varathan, *Water Air Soil Poll.* **234** (2023) 435 (https://doi.org/10.1007/s11270-023-06469-4)
5. S. Wang, Y. Peng, *Chem. Eng. J.* **156** (2010) (https://doi.org/10.1016/j.cej.2009.10.029)
6. K. Shikhaliyev, T. Onsree, A. H. Jaeschke, S. M. Ghoreishian, K. Shariati, A. Martinez, A. Katz, S. Hwang, A. Gaffney, J. M. Urban-Klaehn, J. Lauterbach, *Appl. Catal., B* **337** (2023) 122991 (https://doi.org/10.1016/j.apcatb.2023.122991)
7. M.A. Sadenova, S.A. Abdulina, S. A. Tungatarova, *Clean Technol. Environ.* **18** (2016) 449 (https://doi.org/10.1007/s10098-015-1018-6)
8. M. Kuronen, M. Weller, R. Townsend, R. Harjula, *React. Funct. Polym*. **66** (2006) 1350 (https://doi.org/10.1016/j.reactfunctpolym.2006.03.019)
9. I. Rodriguez-Iznaga, V. Petranovskii, G.Rodriguez-Fuentes, *J. Environ. Chem. Eng.* **2** (2014) 1221 (https://doi.org/10.1016/j.jece.2014.05.012)
10. M. Doula, *Water Res*. **40** (2006) 3167 (https://doi.org/10.1016/j.watres.2009.05.037)

11. M. Doula, A. Dimirkou, *J. Hazard. Mater.* **151** (2008) 738 (https://doi.org/10.1016/j.jhazmat.2007.06.047)
12. A. Dimirkou, *Water Res*. **41** (2007) 2763 (https://doi.org/10.1016/j.watres.2007.02.045)
13. M. Kragović, A. Daković, Ž. Sekulić, M. Trgo, M. Ugrina, J. Perić, G. D. Gatta, *Appl. Surf. Sci.* **258** (2012) 3667 (https://doi.org/10.1016/j.apsusc.2011.12.002)
14. P. Praipipat, S. Jangkorn, P. Ngamsurach, *Environ. Nanotechnol. Monit.* **20** (2023) 100812 (https://doi.org/10.1016/j.enmm.2023.100812)
15. M. T. Mihajlović, S. S. Lazarević, I. M. Janković-Častvan, B. M. Jokić, Đ. T. Janaćković, R. D. Petrović, *Chem. Ind. Chem. Eng. Q*. **20** (2014) 283 (https://doi.org/10.2298/CICEQ121017010M)
16. M. T. Mihajlović, S. S. Lazarević, I. M. Janković-Častvan, J. Kovač, B. M. Jokić, Đ. T. Janaćković, R. D. Petrović, *Clean Technol. Environ. Policy* **17** (2015) 407 (https://doi.org/10.1007/s10098-014-0794-8)
17. P. M. Nekhunguni, N. T. Tavengwa, H. Tutu, *J. Environ. Manage.* **197** (2017) 550 (https://doi.org/10.1016/j.jenvman.2017.04.038)
18. A. Badeenezhad, A. Azhdarpoor, S. Bahrami, S. Yousefinejad, *Mol. Simulat.* **45** (2019) 564 https://doi.org/10.1080/08927022.2018.1564077
19. N. J. Singh, B. Wareppam, A. Kumar, K. P. Singh, V. K. Garg, A. C. Oliveira, L. H. Singh, *J. Mater. Res.* **38** (2023) 1149 (https://doi.org/10.1557/s43578-022-00859-w)
20. S. Mohammadi-Jam, K.E. Waters, *Adv. Colloid Interf. Sci.* **212** (2014) 21 (https://doi.org/10.1016/j.cis.2014.07.002)
21. J. P. Jolivet, E. Tronc, Corinne Chaneac, *C. R. Geoscience* **338** (2006) 488 (https://doi.org/10.1016/j.crte.2006.04.014)
22. F. Rouquerol, J. Rouquerol, K. Sing, *Adsorption by Powders and Porous Solids*, Academic Press, London, 1999 (https://doi.org/10.1016/B978-0-12-598920-6.X5000-3)
23. E. P. Barrett, L. G. Joyner, P. P. Halenda, *J. Am. Chem. Soc.* **73** (1951) 373 (http://dx.doi.org/10.1021/ja01145a126)
24. B. C. Lippens, J. H. de Boer, *J. Catal.* **4** (1965) 319 (https://doi.org/10.1016/0021-9517(65)90307-6)
25. U. Kuila, M. Prasad, *Geophys. Prospec*. **61** (2013) 341 (https://doi.org/10.1111/1365-2478.12028)
26. E. Diaz, S. Ordonez, A. Vega, J. Coca, *J. Chromatogr., A* **1049** (2004) 139 (https://doi.org/10.1016/j.chroma.2004.07.061)
27. C. Bilgic, F.Tumsek, *J. Chromatogr., A* **1162** (2007) 83 (https://doi.org/10.1016/j.chroma.2007.04.003)
28. E. Diez, J.M Gomez, A. Rodriguez, A. Martinez, P. Saez, *Environ. Prog. Sustain.* **39** (2020) e13412 (https://doi.org/10.1002/ep.13412)
29. Y. J. Huang, Y. Jiang, V. R. R. Marthala, B. Thomas, E. Romanova, M. Hunger, *Phys. Chem., C* **112** (2008) 381 (https://doi.org/10.1021/jp7103616).